# Heptane dehydrocyclization over Pt/KL catalysts doped with barium or lanthanum

Javier M. Grau [a], Xosé L. Seoane and Adolfo Arcoya *

*Instituto de Catálisis y Petroleoquímica, CSIC, Cantoblanco, 28049-Madrid, Spain*
*[a] Present address: Instituto de Investigaciones en Catálisis y Petroquímica, INCAPE (UNL, FIQ-CONICET), Santiago del Estero 2654, 3000 Santa Fe, Argentina*

Received 21 March 2002; accepted 8 July 2002

Several 1 wt% Pt/KL catalysts doped with different concentrations of either BaO or $La_2O_3$ were prepared by successive impregnation of a zeolite KL and then characterized by $H_2$–$O_2$ titration, TPR, CO–FTIR, TEM–XEDS and XPS. Catalytic activity measurements in the hydroconversion of *n*-heptane showed that barium highly enhances the aromatization activity of Pt/KL, the more so the higher the barium concentration. The yield to aromatics increases to a lesser degree by adding 1 wt% La, but it is little modified at higher La concentrations. The CO–FTIR results suggest that the promoter effect of barium is related to an electron enrichment of Pt produced by the $BaO \rightarrow Pt^0$ interaction which, according to the TEM–XEDS and XPS results, is more favored than the $La_2O_3 \rightarrow Pt$ interaction.

**KEY WORDS:** KL–zeolite; Pt/KL catalysts; *n*-heptane dehydrocyclization; toluene; barium; lanthanum; CO–FTIR; metal support interaction.

## 1. Introduction

Ever since Bernard [1] reported the high activity of the non-acid Pt/KL catalysts to transform light paraffins into aromatic hydrocarbons, several authors have tried to explain this unique activity. Tauster and Steger [2] proposed that the singular structure of the zeolite KL orients the paraffin molecule in the linear channels in such a way that it favors the terminal C-adsorption and the $C_1$–$C_6$ ring closure on the Pt sites. Other authors [3–5] have attributed the high aromatization activity of the Pt/KL catalysts to electron-rich Pt particles, formed by the interaction of the metal with the basic framework of the zeolite. Iglesia and Baumgartner [6], however, proposed that the aromatizing activity is actually an intrinsic property of the clean platinum surfaces, no matter what the support is. The role of the KL zeolite would be, for these authors, to prevent agglomeration and carbon fouling of the Pt particles within the channels. Triantafillou *et al*. [7] considered, on the other hand, that the high aromatizing selectivity of Pt/KL can be attributed to some combination effects such as size of the Pt clusters, basicity of the zeolite and constrictions imposed by the support pores.

Most of the research works carried out in the past have been devoted to the aromatization of *n*-hexane [8], while those concerning *n*-heptane are more scarce, in spite of the presumable growth of the demand for toluene as a possible substitute for benzene and xylenes in reformulated gasoline. In any case, an improvement in the activity of the catalysts will be necessary in order to make this process economically feasible. A way to obtain this would be, obviously, to enhance the physicochemical properties which are considered to be responsible for the high performance of these catalysts. In a previous work [9] it was reported that the incorporation of $Ba^{2+}$ into the KL zeolite by ion-exchange does not substantially modify either the physicochemical properties or the aromatization activity of a Pt/KL catalyst in the *n*-heptane reaction. The partial exchange of $K^+$ by $La^{3+}$, in contrast, highly decreases the electron density of Pt particles, inhibits the aromatization reaction and promotes the acid activity of the catalyst. These findings prove the negative effect of the acidity on the aromatizing function and, therefore, one can expect that the increase of the zeolite basicity increases the electron density of Pt and promotes the aromatization of *n*-paraffins. To our knowledge, however, few papers devoted to studying the effect of metal oxides on the aromatizing activity of Pt/KL catalysts have been published [10]. With this idea in mind, several portions of a KL-zeolite impregnated with either Ba- or La-nitrates and heated at 873 K to form BaO or $La_2O_3$, respectively, were used as supports of the platinum catalysts in this work. The catalysts were characterized by TPR, gas chemisorption, CO–FTIR, TEM–XEDS and XPS. Their dehydrocyclization activity was evaluated in the reaction of *n*-heptane to toluene, and the results were explained from the electronic state of platinum and the distribution of the catalytic components in the zeolite.

* To whom correspondence should be addressed.
E-mail: aarcoya@icp.csic.es

1011-372X/02/1100-0247/0 

## 2. Experimental

### 2.1. Catalyst preparation

Several fractions of a commercial KL-zeolite (Union Carbide, SK-45; $K_9Al_9Si_{27}O_{72}$, in atoms per unit cell) calcined in air at 873 K for 3 h, pelleted and crushed to 0.6–1.0 mm particle size, were impregnated by the incipient-wetness technique with $Ba(NO_3)_2$ or $La(NO_3)_3{\cdot}6H_2O$ aqueous solutions in an adequate concentration to obtain 1, 3 or 5 wt% of Ba or La. After 24 h at room temperature, the samples were dried at 393 K for 12 h and calcined under air flow at 873 K for 3 h. Then, 1 wt% of Pt was loaded by incipient-wetness impregnation, using aqueous solutions of tetraammineplatinum (II) hydroxide (>99%). The sample CPt, without additives, was prepared by impregnation of the KL-zeolite with the Pt precursor. The catalysts were successively dried at 393 K overnight, calcined at 573 K in an $O_2$ stream and reduced at 773 K under $H_2$ flow, both for 3 h. The reduced samples were stored in a desiccator.

### 2.2. Catalyst characterization

Reducibility of the catalysts was determined by temperature programmed reduction (TPR) in a flow system with a thermal conductivity detector. A sample of 0.5 g of the calcined precursor was outgassed in an argon stream at 373 K for 1 h. After cooling down to room temperature (RT) the carrier gas was switched to a 5% $H_2$/Ar mixture (30 ml $min^{-1}$) and the TPR profile recorded upon heating from RT to 823 K, at 10 K $min^{-1}$.

Platinum dispersion was calculated as $D = 100\,Pt_s/Pt_t$, where $Pt_s$ is the number of exposed platinum atoms per gram of catalyst and $Pt_t$ the total number of platinum atoms per gram of catalyst, as determined by inductively coupled plasma. $Pt_s$ was measured by the $H_2$–$O_2$ titration method in a dynamic system at RT. The samples (0.5 g) were heated at 723 K in a hydrogen stream for 30 min. After evacuation under an argon flow at 573 K for 1 h and cooling down to RT, pulses of $O_2$ (50 $\mu$l) were introduced in the carrier gas until total saturation of the metal surface. Then, the oxygen adsorbed was titrated introducing pulses of hydrogen. From the volume of hydrogen uptake ($H_u$), the number of exposed platinum atoms was calculated assuming an atomic stoichiometry $H_u/Pt_s = 3/1$.

The BET surface area of the supports was measured in a volumetric system, Micromeritics Asap 2000, from the nitrogen adsorption isotherm obtained at 77 K, which includes an estimation of the micropore volume by the *t*-plot method, using the Harkins and Jura *t*-curve. Prior to the measurements the samples (0.2 g) were outgassed at 413 K for 24 h under a helium stream.

The electronic state of platinum was studied by infrared spectroscopy of adsorbed CO. The CO–FTIR spectra were recorded at RT in a Nicolet 5ZDX spectrometer in the range 4800–400 $cm^{-1}$. The self-supported wafer of the reduced sample was treated under hydrogen flow at 723 K for 1 h and outgassed at $10^{-4}$ Pa at the same temperature. After cooling down to RT the IR spectrum was recorded. The sample was then contacted with 4 kPa of CO for 5 min and a new spectrum recorded. The absorption bands of the CO chemisorbed were obtained by subtraction of the spectra. In order to gain information about the location of Pt clusters in the zeolite lattice, new spectra were taken after outgassing at 523 K and $10^{-2}$ Pa for 30 min. For each spectrum (resolution 4 $cm^{-1}$), 128 scans were added.

In order to calculate the intensity of the bands, the experimental spectra were deconvoluted, following the procedure described by Kappers *et al.* [11] for Pt/KL catalysts. The number and position of the band components were estimated by Fourier self-deconvolution (FSD) after base-line correction, with a bandwidth parameter $W = 18\ cm^{-1}$ and an enhancement parameter $K = 2.5$. Using the data given by the interferogram, the original spectra were fitted to a function combining Lorentzian and Gaussian curves in a variable proportion.

Transmission electron microscopy (TEM) was utilized to obtain information about the morphology and distribution of the metal and additive particles in the catalysts. The measurements were carried out in a JEOL JEM 2000FX microscope, 200 kV, provided with an X-ray energy dispersive spectroscopy system (XEDS) with a spatial resolution limit of 4 Å. The catalyst samples were pulverized and dispersed by ultrasonic treatment in 1-butanol. The experimental methodology consisted of making microanalyses in different sectors of the field observed for each sample.

The surface of the catalysts was analyzed by X-ray photoelectron spectroscopy (XPS) with a VG Escalab 200R system, using Mg $K_\alpha$ radiation (1253.6 eV). After reduction, the samples were introduced into the sample holder under isooctane, which was removed during pumping in the preparation chamber of the XPS equipment. The surface atomic ratios of the different species on the catalyst surface were obtained from the integrated intensities, and compares the area of the peaks after background subtraction [12] and specific corrections, using the equation

$$\frac{n_i}{n_j} = \frac{I_i/S_i}{I_j/S_j}\, f(\mathrm{KE}_i, \mathrm{KE}_j) \qquad (1)$$

where $n_i/n_j$ is the atomic ratio between $i$ and $j$ species, $I_i$ and $I_i$ are the intensities of the peaks corresponding to these species and $S$ is the atomic sensitivity factor given by Wagner *et al.* [13]: $S_{Pt} = 2.55$ (4*f* level); $S_{Al} = 0.18$ (2*p* level); $S_{Ba} = 7.9$ (3*d* level); and $S_{La} = 10$ (3*d* level). The function $f(\mathrm{KE}_i, \mathrm{KE}_j)$ is the spectrometer transmission factor, which corrects the detection efficiency when the difference of photoelectron kinetic energy (KE) of $i$ and $j$ is significant. For the spectrometer used in this work that function is $(\mathrm{KE}_i/\mathrm{KE}_j)^{0.5}$ and the values of

KE are: $KE_{Pt} = 1174\,eV$; $KE_{Al} = 1171\,eV$; $KE_{Ba} = 463\,eV$ and $KE_{La} = 412\,eV$.

### 2.3. Catalytic activity measurements

Dehydrocyclization of *n*-heptane was performed in a fixed-bed tubular reactor, containing 2 g of catalyst diluted with SiC, at 723 K, 100 kPa, $H_2/nC_7H_{16} = 7.3$ mol/mol and WHSV = $3.42\,h^{-1}$. A bed of SiC in the reactor above the catalyst bed was employed as a preheater. High-purity hydrogen was successively passed through a Deoxo purifier and a 5A molecular sieve filter. The reactor was heated to 773 K for 1 h under the hydrogen flow required for the reaction and then cooled down to 723 K. Once the system was stabilized the *n*-heptane was fed and the first sample of the reactor effluent collected 15 min later in a condenser at 273 K. Most of the reaction product was collected as condensate at 273 K and analyzed by gas chromatography in a 1,2,3-Tris(2-cyanoethoxy)propane 10 wt% (TCEP)/Chromosorb P column (4 m × 3.18 mm OD) at 353 K. Exit gases were analyzed in two columns: one of TCEP for both the non-condensed gaseous hydrocarbons and the liquid hydrocarbons entrained by the gas flow, and another of powdered activated charcoal, at 313 K, for methane. In order to check the stability of the catalysts, samples of the reactor effluent were periodically taken and analyzed: the liquid samples every 15 min and the gas one every 5 min. From the amount of liquid collected, the exit gas flow and the chromatographic results, the mass balance was made. Reaction data reported in this work fit the carbon balance with an error of ±5%.

Following a conventional methodology [14], two series of experiments were performed with CPt in order to examine possible diffusional effects. (a) At constant WHSV ($3.42\ h^{-1}$), but changing both the liquid *n*-heptane flow and the catalyst weight: 6.84/2, 13.68/4 and 27.36/8 $g\,h^{-1}$/g. The conversion in these cases remained constant. (b) Using different ranges of catalyst particle size: 0.47–0.6, 0.6–1.0, 1.0–1.41 and 1.41–2.38 mm. The conversion increased, going from 1.41–2.38 mm to 1.0–1.41 mm, and then remained constant. So, these results show that under the experimental conditions used in this work, both external and internal diffusional limitations were absent [15].

Coke content of the catalysts after reaction was determined by temperature-programmed oxidation (TPO) in TG equipment, heating 500 mg of sample from RT to 1073 K at $10\,K\,min^{-1}$ in an $O_2$ flow of $100\,ml\,min^{-1}$.

## 3. Results and discussion

### 3.1. Catalyst characterization

Chemical analysis, specific surface area of the supports ($S_g$), metal dispersion ($D$) and average particle size ($d$) are given in table 1. The specific surface area decreases when the additive concentration increases, although the $S_g$ values are high enough to permit a high metal dispersion. Platinum is moderately well dispersed, but it is noticeable that the negative effect of barium on the metal dispersion suggests that it makes the formation of nuclei of Pt crystallites difficult. In contrast, Pt dispersion is not substantially affected by the La addition.

Table 1
Characterization of the catalysts.

| Catalyst | Me (wt%) | $Pt_t$ (wt%) | $S_g$ ($m^2\,g^{-1}$) | $D$ (%) | $d$ (nm) |
|---|---|---|---|---|---|
| CPt | 0.00 | 0.98 | 245 | 42 | 2.14 |
| CBaPt1 | 0.98 | 0.99 | 175 | 40 | 2.25 |
| CBaPt3 | 2.87 | 0.97 | 120 | 34 | 2.64 |
| CBaPt5 | 4.81 | 1.02 | 105 | 24 | 3.75 |
| CLaPt1 | 0.96 | 0.98 | 171 | 41 | 2.19 |
| CLaPt3 | 2.94 | 0.99 | 117 | 44 | 2.04 |
| CLaPt5 | 4.72 | 0.98 | 101 | 43 | 2.09 |

Me, Ba or La; $S_g$, specific surface area; $Pt_t$, Pt loading; $D$, platinum dispersion; $d$, average particle size.

The TPR profiles of the catalyst precursors (figures 1 and 2) show that reduction of Pt occurs below 623 K, indicating that in the conditions used to prepare the catalysts they were completely reduced. The TPR profile of CPt, showing a broad reduction peak at 475 K with a shoulder at 408 K, substantially agrees with that reported by Ostgard *et al.* [16] for a Pt/KL prepared from $Pt(NH_3)_4Cl_2$. This profile was discussed in detail in [9], where, from the atomic ratio $H_u/Pt_t = 1.35$, it was estimated that 65% of platinum is present as $Pt^{2+}$ and 35% as $Pt^{4+}$. The broad peak at 475 K should then

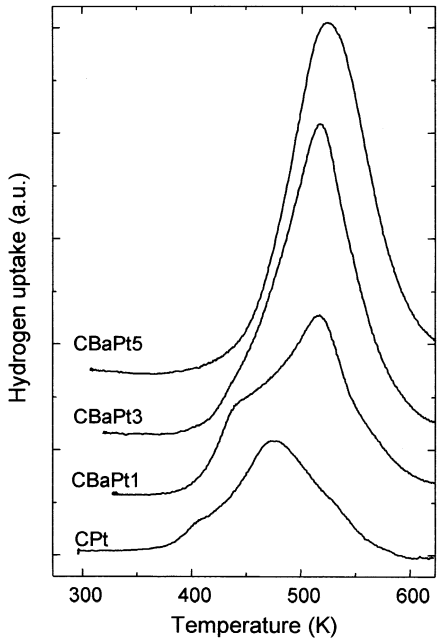


Figure 1. TPR profiles of the CBaPt catalysts.

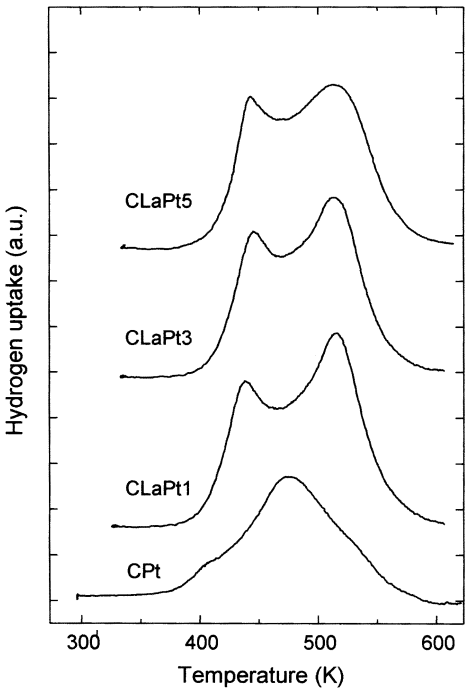


Figure 2. TPR profiles of the CLaPt catalysts.

include the reduction of both PtO and $PtO_2$ species formed during the calcination step. The shoulder at 408 K corresponds to the reduction of $Pt^{2+}$ located on the external surface of the zeolite.

The TPR profiles of Ba-catalysts also exhibit a single broad peak, but at higher temperature than that of CPt (516–523 K), and a shoulder at 440–446 K perceptible for the samples CBaPt1 and CBaPt3. It is remarkable, however, that the hydrogen consumption for these samples is higher than that expected to reach complete reduction of platinum, and it increases as the Ba concentration increases. Since $Ba(NO_3)_2$ was used as precursor, it is probable that the additional consumption of hydrogen is due to the reduction of the remaining $NO_x$ species adsorbed on the support, formed during the calcination step of the catalysts as was observed for other catalysts [17], and in the TPR profile of a KL sample impregnated with $HNO_3$ and calcined at 873 K. On the other hand, the fact that no hydrogen consumption is detected in the TPR measurements of reduced samples indicates that $NO_x$ surface species were removed during the reduction step.

For the La-catalysts two overlapping and broad peaks with maxima at *ca* 440 K and 515 K were recorded. The first one corresponds to the reduction of Pt and the other is probably related to $NO_x$ reduction. For these samples the amount of hydrogen consumed was only slightly higher than the stoichiometric one required to produce Pt metal, indicating that, in this case, most of the $NO_x$ species were removed during the calcination step.

The FTIR spectra of CO adsorbed on the CPt, Ba- and La-catalysts, depicted in figures 3 and 4, exhibit a broad band in the range 2150–1900 $cm^{-1}$, with several

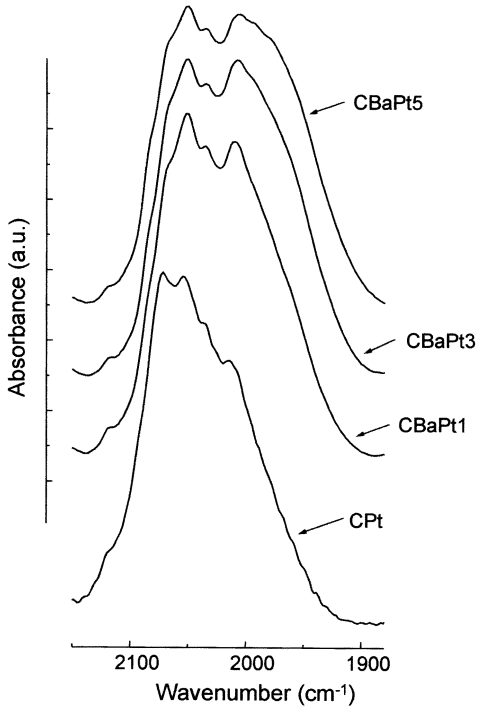


Figure 3. FTIR spectra of CO adsorbed on CBaPt catalysts at room temperature and 4 kPa.

maxima and shoulders corresponding to CO linearly bonded to Pt species in different electronic states [3,4,18]. To analyze these spectra, they were deconvoluted as described in the Experimental Section. As an example, figure 5 shows: (a) the FSD of the experimental

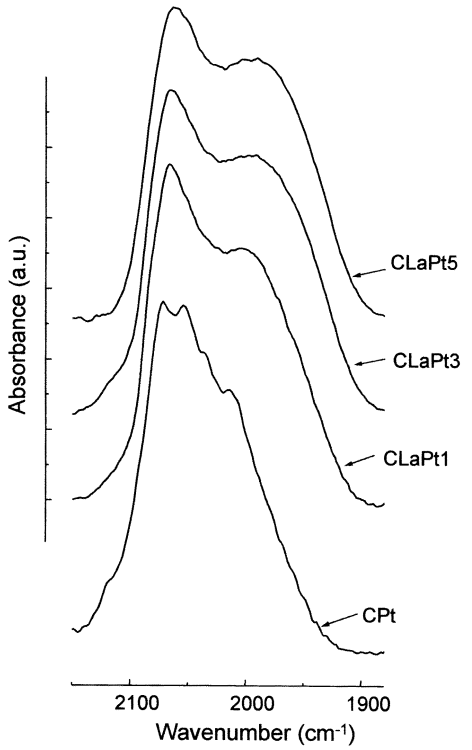


Figure 4. FTIR spectra of CO adsorbed on CLaPt catalysts at room temperature and 4 kPa.

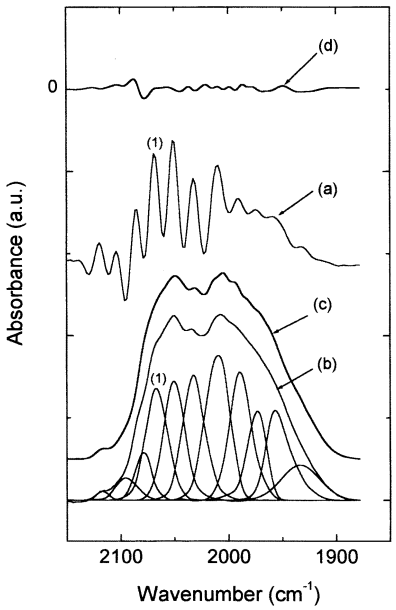


Figure 5. Deconvolution of the CO–FTIR spectra of CBaPt3 catalyst: (a) Fourier self-deconvolution of the experimental spectrum; (b) deconvoluted experimental spectrum with the component bands; (c) the fitted spectrum; and (d) the difference between the deconvoluted measured and fitted spectra.

spectrum; (b) the deconvoluted experimental spectrum with the component bands; (c) the fitted spectrum; and (d) the difference between the deconvoluted measured and fitted spectra, for CBaPt3 catalyst.

The band at 2073 $cm^{-1}$ in the CPt spectrum (figure 3) is associated to CO adsorbed on $Pt^0$ located in the outer surface of the zeolite, while the others at lower wavenumbers are attributed to electron-enriched platinum, probably located within the zeolite but in different environments. The band at 2120 $cm^{-1}$ denotes, on the other hand, the presence of electron-deficient metal atoms [17,19].

The CO–FTIR spectrum of CPt is strongly modified by the presence of Ba (figure 3) and to a lesser degree by La (figure 4). Taking as a reference the band at 2073 $cm^{-1}$ (1 in figure 5), the relative intensity of other bands ($I/I_{2073}$), calculated from the respective areas, is summarized in table 2. For wavenumbers lower than 2000 $cm^{-1}$, $I/I_{2073}$ increases as the Ba content increases, while for the 2120 $cm^{-1}$ band it decreases. These results indicate that an electron enrichment of the Pt particles occurs by the effect of Ba addition. Similar conclusions can be drawn from the IR spectra of the La-doped catalysts (figure 4), although the effect produced by the addition of 3 or 5 wt% of La is less perceptible than that observed for similar concentrations of Ba. These spectral differences suggest that the strength and/or extent of the Ba–Pt interaction is higher than that of La–Pt.

Since the spectra obtained after outgassing the samples at 523 K can be assigned to CO linearly bonded to Pt located inside the channels [18], the progressive shift of the 1962 $cm^{-1}$ band down to 1933 $cm^{-1}$ and its growth, as well as the increase of the 2032 $cm^{-1}$

Table 2
Relative intensity of the FTIR bands of CO chemisorbed on the catalysts.

| Catalyst | $I/I_{2073}$ | | | | |
|---|---|---|---|---|---|
| | 2120 $cm^{-1}$ * | 2034 $cm^{-1}$ * | 2008 $cm^{-1}$ * | 1997 $cm^{-1}$ * | 1963 $cm^{-1}$ * |
| CPt | 0.21 | 0.85 | 0.85 | 0.60 | 0.32 |
| CBaPt1 | 0.10 | 1.14 | 1.34 | 1.03 | 0.71 |
| CBaPt3 | 0.06 | 1.13 | 1.40 | 1.16 | 0.91 |
| CBaPt5 | 0.05 | 1.13 | 1.37 | 1.17 | 1.00 |
| CLaPt1 | 0.07 | 0.67 | 0.93 | 0.61 | 0.46 |
| CLaPt3 | 0.07 | 0.81 | 0.97 | 0.78 | 0.68 |
| CLaPt5 | 0.06 | 0.82 | 1.04 | 0.82 | 0.76 |

Me, Ba or La; $I/I_{2073}$, intensity of FTIR bands relative to the 2073 $cm^{-1}$ one.
* Wavenumber.

band with the Ba concentration (figure 6), are consistent with the parallel increase of both the electron density of Pt within the channels and its population, as was suggested above. In a similar way the lower shift and intensity of those bands shown in figure 7 for La-doped catalysts agree with a lower electron enrichment of Pt.

### 3.2. Dehydrocyclization activity

Performances of the catalysts in the hydroconversion of *n*-heptane at 723 K after 15 min of reaction are given in table 3. In addition to toluene and benzene (*T* and *B*), heptane isomers (*i*-$C_7$), methane ($C_1$), hydrocracking products ($C_2$–$C_6$), cycloalkanes ($CC_5$–$CC_6$) and heptenes

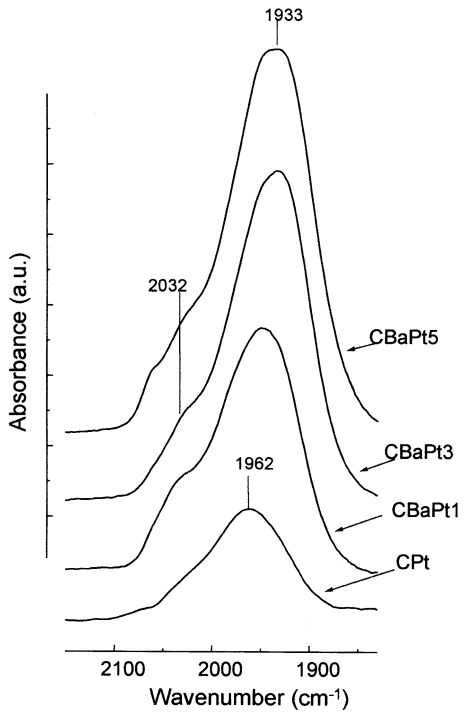


Figure 6. FTIR spectra of CO remaining on the CBaPt catalysts upon adsorption at room temperature and 4 kPa and subsequent evacuation at 523 K and $10^{-2}$ Pa.

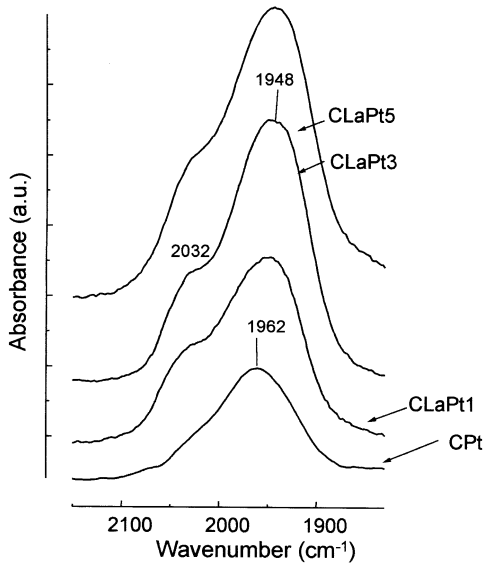


Figure 7. FTIR spectra of CO remaining on the CLaPt catalysts upon adsorption at room temperature and 4 kPa and subsequent evacuation at 523 K and $10^{-2}$ Pa.

($C_7^=$) were obtained. Conversion ($X$) is defined as a percentage of *n*-heptane fed to the reactor transformed into products and yielding to a product $i$, ($Y_i$) as the number of *n*-heptane molecules transformed into $i$ per 100 molecules of *n*-heptane fed.

As shown in table 3, the addition of 1 wt% of Ba improves the yield of both aromatization ($Y_T + Y_B$) and hydrogenolysis products ($Y_{C_1}$ and $Y_{C_2-C_6}$), as compared with the reference catalyst (CPt), but decreases the $Y_{i\text{-}C_7}$, the last indicating a decrease in the number of the acid sites. When the Ba loading increases, a significant enhancement of the aromatization yields and *TOF* is observed, reaching 46.9% and 347 $s^{-1}$, respectively, for a 5 wt% Ba content. The addition of 1 wt% of La also improves the aromatization performances of Pt/KL, but to a lesser degree than Ba. In contrast, the effect of 3 or 5 wt% of La is hardly perceptible. It is interesting to point out, however, that the aromatization yields ($Y_T + Y_B$) of La-catalysts are much higher than that reported elsewhere (2.4%) for a PtLa/KL catalyst, but where lanthanum was incorporated by ion exchange [9].

Since Ba and La precursors were incorporated into the zeolite by impregnation, it is reasonable to assume that upon calcination at 873 K they were mainly transformed into BaO and $La_2O_3$, respectively. So, in samples containing Ba, due to the strong basic character of BaO, an electron transfer towards Pt through the interface BaO–Pt could explain the electronic enrichment of Pt, which increases as the Ba loading increases, as evidenced by the CO–FTIR spectra. On the other hand, since the greater the Ba loading the higher the yield of aromatics, one can assert that an increase in the amount of the electron-enriched Pt ($Pt^{\delta-}$) results in higher dehydrocyclization activity, as shown in table 3. This effect of Ba contrasts with that reported by Gao *et al.* [10], who found that aromatization of *n*-hexane progressively decreases when the Ba content in the catalyst increases, in the range 1–5 wt%. The differences in the nature of the Pt precursors and the catalyst preparation conditions can probably explain this discrepancy.

The fact that lanthanum does not parallel the catalytic effect of barium indicates that the aromatization of *n*-heptane is scantly sensitive to the concentration of lanthanum, which is consistent with the exiguous changes of the electron density of Pt suggested by the CO–FTIR spectra given in figures 4 and 6. Since BaO and $La_2O_3$ are basic in nature, the unexpected behavior of the latter could be related to its distribution in the catalyst, which can be different from that of BaO. In order to gain information about this subject, the samples CBaPt3 and CLaPt3 were examined by TEM–XEDS. Micrographs of both samples showed Pt crystallites smaller than 3 nm, without any appreciable difference being observed. The XEDS spectra display, however, remarkable differences between the distribution of the

Table 3
Dehydrocyclization activity of the catalysts at $T = 723$ K; $P = 100$ kPa; WHSV = 3.42 $h^{-1}$ and $H_2$/n-$C_7$ = 7.3 mol/mol.

| Catalyst | CPt | CBaPt1 | CBaPt3 | CBaPt5 | CLaPt1 | CLaPt3 | CLaPt5 |
|---|---|---|---|---|---|---|---|
| $X$ (%) | 30.7 | 42.5 | 56.5 | 58.5 | 35.9 | 32.3 | 30.6 |
| $10^3$ TOF ($s^{-1}$) | 135 | 196 | 307 | 433 | 162 | 139 | 126 |
| $Y_T$ (%) | 13.3 | 21.1 | 34.3 | 40.9 | 16.1 | 15.0 | 14.5 |
| $Y_B$ (%) | 1.7 | 5.0 | 8.0 | 6.0 | 3.3 | 3.0 | 2.6 |
| $Y_{C_2-C_6}$ (%) | 3.7 | 6.2 | 5.4 | 2.9 | 5.4 | 5.2 | 4.9 |
| $Y_{iC_7}$ (%) | 2.2 | 1.1 | 0.9 | 0.8 | 1.2 | 1.1 | 1.0 |
| $Y_{C_7^=}$ (%) | 3.2 | 2.0 | 2.1 | 1.5 | 2.6 | 2.4 | 2.2 |
| $Y_{CC_5-CC_6}$ (%) | 6.9 | 3.5 | 2.9 | 3.0 | 3.4 | 3.3 | 3.4 |
| $Y_{C_1}$ (%) | 1.6 | 3.7 | 2.8 | 3.4 | 3.9 | 2.4 | 2.2 |
| $10^3$ $TOF_{(T+B)}$ ($s^{-1}$) | 66 | 120 | 230 | 347 | 88 | 77 | 70 |
| $R$ | 0.48 | 0.60 | 0.62 | 0.67 | 0.59 | 0.60 | 0.63 |
| Coke (wt%)* | 0.60 | 0.46 | 0.33 | 0.25 | 0.50 | 0.39 | 0.32 |

$X$, *n*-heptane conversion; TOF, turnover frequency; $Y$, yield; $S$, selectivity; $R$, remaining aromatization activity.
* Coke content of the catalysts after 240 min on stream.

Table 4
XEDS analysis of CBaPt3. Representative values of Ba and Pt concentration in different zones of the sample.

| Zone | Chemical composition (mol%) | |
|---|---|---|
| | Ba | Pt |
| 1 | 1.54 | 0.00 |
| 2 | 1.51 | 0.37 |
| 3 | 5.56 | 7.77 |
| 4 | 2.10 | 0.18 |
| 5 | 1.54 | 0.00 |
| 6 | 1.61 | 0.34 |
| 7 | 1.21 | 0.15 |
| 8 | 1.50 | 5.01 |
| 9 | 1.34 | 0.86 |
| 10 | 2.08 | 1.02 |

Table 5
XEDS analysis of CLaPt3. Representative values of La and Pt concentration in different zones of the sample.

| Zone | Chemical composition (mol%) | |
|---|---|---|
| | La | Pt |
| 1 | 0.00 | 8.00 |
| 2 | 1.13 | 0.24 |
| 3 | 30.03 | 0.80 |
| 4 | 0.00 | 0.00 |
| 5 | 0.99 | 0.38 |
| 6 | 19.59 | 0.02 |
| 7 | 21.73 | 0.63 |
| 8 | 0.44 | 0.18 |
| 9 | 0.08 | 0.00 |
| 10 | 2.40 | 0.05 |

catalytic components of the two samples. The results summarized in tables 4 and 5, as representative examples of the large number of microanalyses performed for CBaPt3 and CLaPt3, show that the signal of Ba, in contrast with that of La, was weak but constant in all the fields analyzed. From these results one can deduce that Ba is highly disperse and well distributed throughout the zeolite. The XEDS measurements evidenced, moreover, the presence of Pt clusters, which were not observed by TEM, probably due to the fact that they are extremely small (<1 nm). In this sample, because Pt is always in the close vicinity of Ba, it can be expected that the extent of the electron transfer from BaO to Pt increases with the Ba loading and, consequently, the fraction of $Pt^{\delta-}$ also increases, as shown by FTIR. For CLaPt3, however, the XEDS results (table 5) suggest that La is heterogeneously distributed and, moreover, most Pt and La particles are segregated and only part of the metal is close to La. These results support the hypothesis that the greater the $Pt^{\delta-}$ fraction the higher the aromatizing activity. These findings agree with those found by Miller *et al*. [20] in the *n*-hexane aromatization, using a catalyst of Pt deposited on an alkalized K–LTL zeolite.

The fact that the average size of the Pt crystals given in table 1 is larger than the dimensions of the cavities ($0.48 \times 1.24 \times 1.07$ nm) and windows (0.71 nm) of the zeolite, together with the presence of very small particles of Pt, evidenced by TEM–XEDS, suggests a bimodal distribution of the Pt particle size in the zeolite, *i.e*., Pt clusters inside the channels and Pt crystals on the external surface. Similar results were found by Han *et al*. [4], among other authors, for Pt/KL catalysts. In order to get a better insight on the chemical state of the catalyst surface, all the samples were analyzed by XPS and the atomic surface ratios calculated using equation 1 (table 6). Following the literature [21,22] we have used these ratios to know the distribution of Pt, Ba and La in the catalyst grains. According to the arguments given elsewhere [23], the values of XPS surface atomic ratios La/Al, higher than those of the bulk ratios listed in table 6, are consistent with a preferential deposition of La on the external surface of the catalysts. On the other hand, the XPS Ba/Al values, which are only slightly higher than those of the bulk, indicate that Ba is more uniformly distributed. Furthermore, since the XPS values of Ba/Al are lower than those of La/Al for the same additive concentration, it is reasonable to assume that the fraction of Ba inside the zeolite is higher than that of La. In a similar way the XPS values of Pt/A indicate that platinum is reasonably well distributed in the Ba-catalysts, while it is preferentially deposited outside in the La-catalysts, suggesting that lanthanum makes difficult the access of Pt into the zeolite channels. Therefore, we believe that the higher electron density of Pt clusters in the Ba-catalysts is due to the higher basicity inside the channels derived from the presence of well-distributed BaO, which interacts with platinum atoms either directly or through the $O^{2-}$ anions of the lattice.

Since the activity of the catalysts decays as a function of time on stream until reaching a pseudo-steady-state, we have defined the residual aromatization activity ($R$) as the ratio between the $TOF_{(T+B)}$ after 240 min and

Table 6
Surface atomic ratios of the catalysts.

| Catalyst | Pt/Al [a] | | Ba/Al [a] | | La/Al [a] | |
|---|---|---|---|---|---|---|
| | XPS | Bulk | XPS | Bulk | XPS | Bulk |
| CPt | 0.0175 | 0.0139 | | | | |
| CBaPt1 | 0.0172 | 0.0141 | 0.0289 | 0.0198 | | |
| CBaPt3 | 0.0160 | 0.0138 | 0.0616 | 0.0580 | | |
| CBaPt5 | 0.0158 | 0.0145 | 0.1163 | 0.0972 | | |
| CLaPt1 | 0.0265 | 0.0139 | | | 0.0559 | 0.0192 |
| CLaPt3 | 0.0287 | 0.0141 | | | 0.1252 | 0.0588 |
| CLaPt5 | 0.0290 | 0.0140 | | | 0.1833 | 0.0944 |

[a] Atom/atom.

Table 7
Dehydrocyclization activity of the catalysts at $T = 723\,K$; $P = 500\,kPa$; $WHSV = 3.42\,h^{-1}$ and $H_2/n\text{-}C_7 = 7.3\,mol/mol$.

| Catalyst | CPt | CBaPt3 | CLaPt5 |
|---|---|---|---|
| $X$ (%) | 88.9 | 86.2 | 83.7 |
| $10^3$ TOF ($s^{-1}$) | 391 | 469 | 360 |
| $Y_T$ (%) | 42.2 | 48.4 | 42.8 |
| $Y_B$ (%) | 4.8 | 4.8 | 4.1 |
| $Y_{C_2-C_6}$ (%) | 21.8 | 12.4 | 18.7 |
| $Y_{C1}$ (%) | 6.2 | 3.5 | 5.1 |
| $10^3$ $TOF_{(T+B)}$ ($s^{-1}$) | 207 | 289 | 202 |
| $R$ | 0.93 | 0.94 | 0.94 |
| Coke* (wt%) | 0.09 | 0.04 | 0.06 |

$X$, $n$-heptane conversion; TOF, turnover frequency; $Y$, yield; $S$, selectivity. $R$, remaining aromatization activity.
* Coke content of the catalysts after 240 min on stream.

15 min on stream. The values of $R$ (table 3) for the doped catalysts are higher than for CPt and they increase as the additive concentration increases. These results are consistent with the coke content on the catalysts after reaction, which decreases as the Ba or La content increases.

At this point, and following Iglesia and Baumgartner [6], one can reasonably ask if the Ba- and La-catalysts are more aromatizing because the additives either produce a specific promoter effect or inhibit their deactivation. In an attempt to answer this question the activity of samples CPt, CBaPt3 and CLaPt3 was evaluated at 500 KPa. At this pressure, the deactivation of Pt by coke should be very low [24].

The results in table 7 compared with those in table 3 show that, for the three catalysts, the yields to aromatics increase and get closer together, while the amount of coke in the used samples decreases. From these results, it seems that at atmospheric pressure CBaPt and CLaPt catalysts are more aromatizing than CPt because BaO and $La_2O_3$ produce an effect which is similar to that produced by an increase in the $H_2$ pressure, *i.e.*, they diminish the carbon formation because they neutralize acid sites. However, if one examines in detail the data of table 7 (TOF, for example), it appears that the beneficial effect of BaO goes beyond the simple inhibition of coke formation. So, in addition to this effect, our results indicate that Ba increases the yield to toluene + benzene and decreases that of the other products of reaction. This means that for Ba-catalysts both effects of BaO, namely, inhibition of coke and electronic promotion of Pt within the zeolite, positively cooperate in the dehydrocyclization of *n*-heptane.

## 4. Conclusions

Several Pt/KL catalysts doped with Ba or La have been prepared and characterized and their dehydrocyclization activity evaluated in the conversion of *n*-heptane at 723 K in a fixed-bed reactor. It has been shown that the surface properties as well as the catalytic performance are substantially modified by $Ba(NO_3)_2$ and $La(NO_3)_3{\cdot}6H_2O$ addition. Most of the BaO formed during the calcination step of the catalysts is very well dispersed and distributed throughout the zeolite, and it does not hinder the access of Pt to the channels. The barium oxide within the zeolite produces an electron-enrichment of the Pt clusters, observed by FTIR, either by direct $BaO \rightarrow Pt^0$ interaction or through the $O^{2-}$ anions of the lattice. $La_2O_3$, in contrast, is preferentially deposited on the external surface of the zeolite and partially segregated from the platinum particles. Under these conditions, lanthanum hinders the accessibility of Pt to the zeolite channels and the fraction of electron-enriched Pt produced is lower than for the Ba-catalysts. We believe that the higher fraction of $Pt^{\delta-}$ present inside the L-channels in the Ba-catalysts is the reason for their higher aromatizing performance as compared to their counterpart La-catalysts.

## Acknowledgments

The authors gratefully acknowledge financial support from CICYT, Spain (Projects MAT98-1091 and MAT1999-0812), and JMG also thanks CONICET and UNL, Argentina, for the Ph.D. fellowship (Project FOMEC 824). The authors also thank Prof. J.L.G. Fierro for providing the XPS spectra and for helpful discussions.

## References

[1] J.R. Bernard, in: *Proc. 5th Int. Conf. Zeolites*, ed. L.W. Rees (Heyden, London, 1980), p. 686.
[2] S.J. Tauster and J.J. Steger, J. Catal. 125 (1990) 387.
[3] C. Besoukhanova, J. Guidot, D. Barthomeuf, M. Breysse and J.R. Bernard, J. Chem. Soc. Faraday Trans. 77, 1 (1981) 1595.
[4] W. Han, A.B. Kooh and R.F. Hicks, Catal. Lett. 18 (1993) 219.
[5] P.V. Menacherry and G.L. Haller, J. Catal. 177 (1998) 175.
[6] E. Iglesia and J.E. Baumgartner, Stud. Surf. Sci. Catal. 75 (1993) 993.
[7] N.D. Triantafillou, J.T. Miller and B.C. Gates, J. Catal. 155 (1995) 131.
[8] P. Mériaudeau and C. Naccache, Catal. Rev.-Sci. Eng. 39, 18-2 (1997) 5.
[9] M. Grau, L. Daza, X.L. Seoane and A. Arcoya, Catal. Lett. 53 (1998) 161.
[10] Z. Gao, X. Jiang, Z. Ruan and Y. Xu, Catal. Lett. 19 (1993) 81.
[11] M.J. Kappers, J.T. Miller and D.C. Koningsberger, J. Phys. Chem. 100 (1996) 3227.
[12] G.L. Ott, T.H. Fleisch and W.N. Delgass, J. Catal. 70 (1979) 394.
[13] C.D. Wagner, L.E. Davis, M.V. Zeller, J.A. Taylor, R.H. Raymond and L.H. Gale, Surf. Interface Anal. 3 (1981) 211.
[14] O. Levenspiel, *Chemical Reaction Engineering*, Chapter 14 (J. Wiley, New York, 1966).
[15] J.M. Grau, *"Study of the catalysts and the mechanism of dehydrocyclization of n-heptane into toluene over P/KL catalysts modified by barium and lanthanides"*, PhD Thesis, Universidad Autónoma de Madrid, Madrid, Spain, 1999.

[16] D.J. Ostgard, L. Kustov, K.R. Poeppelmeier and W.M.H. Sachtler, J. Catal. 133 (1992) 342.
[17] X.L. Seoane, N.S. Fígoli, P. L'Argentiere, J.A. González and A. Arcoya, Cat. Lett. 47 (1997) 213.
[18] A. Yu Stakheev, E.S. Shpiro, N.I. Jaeger and G. Schulz-Ekloff, Catal. Lett. 34 (1995) 293.
[19] W. Juszczyk, Z. Karpiski, I. Ratajczykowa, Z. Stanasiuk, J. Zielinski, L.L. Sheu and W.M.H. Sachtler, J. Catal. 120 (1989) 68.
[20] J.T. Miller, N.G.B. Agrawal, G.S. Lane and F.S. Modica, J. Catal. 163 (1996) 106.
[21] J.S. Brinen and J.L. Schmitt, J. Catal. 45 (1976) 274.
[22] W.N. Delgass, G.L. Haller, R. Kellerman and J.H. Lunsford, *Spectroscopy in Heterogeneous Catalysis* (Academic Press, New York, 1979) Chap. 8, p. 267.
[23] L.M[a]. Gómez-Sainero, A. Arcoya and X.L. Seoane, Ind. & Eng. Chem. Res. 39 (2000) 2849.
[24] A.B. Kooh, W. Han and R.F. Hicks, Catal. Lett. 18 (1993) 209.